On the Differences in Ablation Seasons of Arctic and Antarctic Sea Ice

EDGAR L. ANDREAS AND STEPHEN F. ACKLEY

U.S. Army Cold Regions Research and Engineering Laboratory, Hanover, NH 03755

(Manuscript received 26 May 1981, in final form 30 September 1981)

ABSTRACT

Arctic sea ice is freckled with melt ponds during the ablation season; Antarctic sea ice has few, if any. On the basis of a simple surface heat budget, we investigate the meteorological conditions necessary for the onset of surface melting in an attempt to explain these observations. The low relative humidity associated with the relatively dry winds off the continent and an effective radiation parameter smaller than that characteristic of the Arctic are primarily responsible for the absence of melt features in the Antarctic. Together these require a surface-layer air temperature above 0°C before Antarctic sea ice can melt. A ratio of the bulk transfer coefficients C_H/C_E less than 1 also contributes to the dissimilarity in Arctic and Antarctic ablation seasons. The effects of wind speed and of the sea-ice roughness on the absolute values of C_H and C_E seem to moderate regional differences, but final assessment of this hypothesis awaits better data, especially from the Antarctic.

1. Introduction

Sea-ice ablation processes in the Arctic and in the Antarctic are distinctly different. In the Arctic, as the days get longer and the air temperature warms, melt ponds form on the ice and the surface loses its homogeneity (e.g., Nansen, 1897). Because the albedo of these melt ponds is lower than the albedo of the surrounding ice (Langleben, 1969, 1971), the ponds themselves then enhance the melting process. Antarctic sea ice, on the other hand, shows little surface ablation and rarely, if ever, has melt ponds. Arctowski (1908), for example, reported no melt ponds during the drift of the *Belgica* in the Bellingshausen Sea. During the northward drift of the *Endurance* across the Weddell Sea, Wordie (1921) noted that the absence of melt ponds was the conspicuous difference between Arctic and Antarctic sea ice. Spichkin (1966) likewise emphasized the absence of surface melting at Mirny, on the other side of the continent, and Ackley (1979) recently confirmed, through field work and from Landsat images, that there is no surface melting in the Weddell Sea. The surface albedo of Antarctic sea ice is consequently near that typical of snow-covered ice year around.

This difference between the ablation seasons in the Arctic and in the Antarctic must result from differences in the meteorological variables driving the surface energy budget. For example, because in the spring Antarctic surface winds are 60–100% stronger than Arctic winds, we suspect that the magnitude of the turbulent transfer may effectively preclude surface melting in the Antarctic—or perhaps it is the difference in humidity (Spichkin, 1966). The relatively dry winds off the continent lead to a relative humidity in the surface layer over Antarctic sea ice that is generally 60% or less, while springtime humidity over Arctic sea ice is typically >75%. This humidity difference will again enhance turbulent surface transfer in the Antarctic.

In this paper, by looking at a simple surface energy budget, we will attempt to better determine which meteorological variables are responsible for the difference between Arctic and Antarctic spring sea-ice characteristics. We will show that the energy budget of a sea-ice surface at the onset of melting can be balanced in the Antarctic only when the surface-layer air temperature is above freezing; while in the Arctic a balance is possible with the air temperature below freezing. The lower relative humidity in the Antarctic is, indeed, largely responsible for this difference; a dimensionless effective radiation parameter ϕ that is larger in the Arctic than in the Antarctic is important, too; and a ratio of the bulk transfer coefficients for sensible and latent heat C_H/C_E less than one also contributes.

2. The surface energy budget

We write the energy budget of a thin layer at the sea-ice surface at the start of the ablation season as

$$Q_n - C = F_H + F_E + L_f \frac{dm}{dt} . \qquad (1)$$

Our sign convention for the fluxes is that used by Munn (1966): the net radiative flux Q_n is positive when the surface is gaining energy; a positive conductive flux C means that heat is conducted down into the ice (or snow); and the turbulent sensible (F_H) and latent (F_E) heat fluxes are both upward when positive. The remaining term in (1) reflects surface melting: L_f is the latent heat of fusion of water and m is the mass of water formed per unit surface area by the melting of ice or snow; so $L_f(dm/dt)$ is the energy consumed by melting. We need not include a heat storage term in (1) because the ice layer we are considering has little heat storing capacity: not only is it thin, but at the onset of ablation it is at its freezing point and virtually isothermal.

To investigate why there is no surface melting in the Antarctic, we look at (1) just before melting occurs. Then

$$Q_n - C - F_H - F_E = 0. \quad (2)$$

We make a bulk parameterization of the turbulent fluxes

$$F_H = C_H \rho c_p U[T_s - T_a], \quad (3)$$

$$F_E = C_E \rho L_v U[q_{sat}(T_s) - f q_{sat}(T_a)]. \quad (4)$$

Here ρ is the density of air; c_p its specific heat at constant pressure; L_v the latent heat of sublimation of ice; U the wind speed at, say, a 10 m reference height; T_a the air temperature at that height; T_s the surface temperature; $q_{sat}(T)$ the saturation specific humidity at temperature T; f the relative humidity; and C_H and C_E are bulk transfer coefficients.

Because the surface is on the verge of melting, we can make several simplifications in Eqs. (3) and (4). Just prior to melting $T_s = 0°C$. We use Murray's (1967) method of calculating specific humidity. For an atmospheric pressure of 1013.25 mb this is

$$q_{sat}(T) = q_0 \exp[aT/(T + 273.15 - b)] = q_0\, g(T), \quad (5)$$

where $q_0 = 3.747 \times 10^{-3}$ kg kg^{-1}, T is in °C, and $a = 17.2693882$ and $b = 35.86$ for saturation with respect to water, or $a = 21.8745584$ and $b = 7.66$ for saturation with respect to ice. With these substitutions in Eqs. (3) and (4), Eq. (2) becomes

$$Q_n - C + C_H \rho c_p U T_a - C_E \rho L_v q_0 U[1 - f g(T_a)] = 0. \quad (6)$$

A quick algebraic manipulation then shows that if there is to be no melting, the relative humidity must obey

$$f = g^{-1}(T_a)\left[1 - \frac{Q_n - C}{C_E \rho L_v q_0 U} - \frac{C_H}{C_E}\frac{c_p T_a}{L_v q_0}\right]. \quad (7)$$

The terms in brackets on the right-hand side of Eq. (7) are all dimensionless. We define a parameter ϕ equal to the second term in brackets in (7),

$$\phi = \frac{Q_n - C}{C_E \rho L_v q_0 U}. \quad (8)$$

This is the ratio of the nonturbulent flux to the maximum possible value of the latent heat flux: that is, the latent heat flux that would obtain if the relative humidity were zero. ϕ, in essence, parameterizes the effective net radiation at the surface. For example, if U is large, the rapid removal of heat by surface sublimation can preclude melting despite a large net radiation balance. On the other hand, if U is small and there is thus little latent heat loss, even a small, positive radiation balance may lead to melting.

In the next section we use Eq. (7) to investigate the effects of f, T_a, ϕ and C_H/C_E on the surface energy budget just prior to melting; but we must first consider the value of Q_n.

The net radiation Q_n is the crucial element in the specification of ϕ. Consistent measurements of Q_n in the Arctic and the Antarctic are scarce, however, and existing numerical computations of it are based on such a host of models and assumptions that estimating ϕ from these sources is of dubious value. Therefore, to obtain consistent and comparable values of ϕ, we will estimate Q_n at the start of the ablation seasons in both the Arctic and the Antarctic.

The net radiation is the sum of shortwave and longwave components,

$$Q_n = Q_s(1 - \alpha) - Q_L, \quad (9)$$

where Q_s is the incoming shortwave radiation, α is the surface albedo, and Q_L is the net longwave radiation. Langleben (1966) used the rapid decrease in surface albedo to designate the start of the Arctic ablation season; the date is typically 1 June. Although there is not a similar ablation indicator in the Antarctic, an equivalent date in the seasonal progression is 1 December. Let us, therefore, estimate Q_n for 1 June at 80°N and for 1 December at 70°S. 80°N is in the central Arctic, and 70°S is a latitude representative of the Weddell, Bellingshausen, and Amundsen Seas and of the Ross Sea sector.

We compute the clear sky global radiation, Q_{s0}, from Zillman's (1972) formula (see also Pease, 1975; Parkinson and Washington, 1979),

$$Q_{s0} = \frac{S_e \sin^2 A}{(\sin A + 2.7)10^{-3} e_a + 1.085 \sin A + 0.100}. \quad (10)$$

In (10) S_e is the extraterrestrial solar beam irradiance based on a solar constant S_0 of 1353 W m^{-2},

$$S_e = S_0/r^2, \quad (11)$$

where r is the ratio of actual to mean Earth–Sun distance; A is the solar altitude, which can be found from

$$\sin A = \sin\theta \sin\delta + \cos\theta \cos\delta \cos\eta, \quad (12)$$

TABLE 1. The computation of net radiation.

Parameters	Arctic (1 June)	Antarctic (1 December)
θ	80°N	70°S
δ	21.95°	−21.68°
A_n	31.88°	41.68°
r	1.01405	0.98604
S_e (W m^{-2})	1316	1392
e_a (mb)	4.89	3.66
c	0.75	0.75
α	0.6	0.6
Flux terms (W m^{-2})		
$\bar{Q}_{s0}$	348	356
Q_s	207	219
$Q_s(1-\alpha)$	83	87
$Q_{L\uparrow}$	306	306
$Q_{L\downarrow}$	206	200
Q_L	40	42
Q_n	43	45

where θ is the latitude, δ is the solar declination, and η is the hour angle (see List, 1963); e_a is the vapor pressure (in mb) of the air. We will show later that the air temperature is near 0°C when surface melting begins; consequently, because variations in the value of e_a are not critical in (10), we use values of e_a based on typical relative humidities at 0°C. In the Arctic $e_a = 4.89$ mb (80% × 6.1078 mb) and in the Antarctic $e_a = 3.66$ mb (60% × 6.1078 mb). To obtain a climatological value of the global radiation $\bar{Q}_{s0}$, we average (10) over a full day, integrating in 30 min steps—a method similar to that used by Parkinson and Washington (1979) and Hibler (1980). This integration is straightforward since the Sun does not set on 1 June at 80°N or on 1 December at 70°S.

The cloud cover and the solar altitude determine the shortwave radiation actually available at the surface. We estimate incoming solar radiation from (Reed, 1977)

$$Q_s = \bar{Q}_{s0}(1 - 0.62c + 0.0019A_n), \qquad (13)$$

where c is the cloud cover in tenths and A_n is the noon solar altitude in degrees. c is 0.75 in both the Arctic on 1 June (Parkinson and Washington, 1979) and the Antarctic on 1 December [Parkinson and Washington (1979) from van Loon (1972)].

Langleben (1966, 1971) showed that in the Arctic the surface albedo α is roughly 0.6 just prior to melting. Weller (1968a,b) measured somewhat smaller albedo values of 0.4–0.5 in November in the Antarctic; but because the ice at his coastal site was periodically swept clean of snow by katabatic winds, we suspect his numbers may be lower than open sea values. Consequently, we use $\alpha = 0.6$ for both the Arctic and the Antarctic just before melting begins.

We now turn to the longwave contribution to Eq. (9). The longwave surface emission is

$$Q_{L\uparrow} = \epsilon\sigma T_s^4, \qquad (14)$$

where T_s is the surface temperature (273.15 K), σ is the Stefan-Boltzmann constant, and ϵ is the surface emissivity, 0.97 (Kondratyev, 1969; Pease, 1975; Hibler, 1980).

The clear-sky downward longwave flux depends on the humidity and surface-layer air temperature. Idso (1981) gave

$$Q_{L\downarrow} = \epsilon\epsilon_a\sigma T_a^4, \qquad (15)$$

where, in general,

$$\epsilon_a = 0.700 + 5.95 \times 10^{-5} e_a \exp(1500/T_a). \qquad (16)$$

Because of the lower aerosol concentrations in remote areas, Eq. (16) seems to overestimate the effective emissivity there by 0.099, however (Idso, 1980). For the Arctic and the Antarctic we thus use

$$\epsilon_a = 0.601 + 5.95 \times 10^{-5} e_a \exp(1500/T_a) \qquad (17)$$

in (15). As we mentioned, since T_a will be near T_s at the onset of melting, we simplify (15) and (17)—with minimal effect on the computed radiation balance—by substituting T_s for T_a.

The net longwave radiation also is influenced by clouds. Kondratyev (1969, p. 577) recommended a cloud factor of $(1 - 0.8c)$ for the warm half of the year at latitudes above 60°. The net longwave radiation is thus

$$Q_L = (Q_{L\uparrow} - Q_{L\downarrow})(1 - 0.8c). \qquad (18)$$

Table 1 lists the values of Q_n computed from (9) and shows parameters and some of the intermediate steps in the computation. Despite the difference in latitudes, the values of the net radiation in the Arctic and the Antarctic are similar because the values of $\bar{Q}_{s0}$ turn out to be similar. Though the noon Sun is higher in the sky at 70°S than at 80°N, the midnight Sun remains higher in the north than in the south. Averaging over a day smooths out these hourly extremes and yields more representative values of the shortwave flux.

3. Results

Spring winds in the surface layer over Arctic sea ice are generally 4–6 m s^{-1} (Vowinckel and Orvig, 1970; Thorpe *et al.*, 1973; Johnson, 1976; Brower *et al.*, 1977; Banke *et al.*, 1980), while Antarctic winds are somewhat stronger, 7–10 m s^{-1} (Weller, 1968a, 1968b; Schwerdtfeger, 1970). With these values, with $C_E = 1.4 \times 10^{-3}$, and with the values of Q_n shown in Table 1, a range of ϕ values for 1 June in the Arctic is [0.4, 0.6] and for 1 December in the Antarctic is [0.2, 0.4]. To obtain these values we have taken C to be zero in Eq. (8): since $T_s = 0$°C, the ice will be virtually isothermal so C will be negligible.

Our estimated values of Q_n and these computations of ϕ put us at odds with Spichkin (1966), who stated (without references) that the radiation balance in the Antarctic is twice what it is in the Arctic and that Antarctic winds are twice the strength of Arctic winds. He would thus compute identical ϕ values for the two regions. Our computations suggest, on the other hand, that in the Arctic the net radiation is relatively more important in the surface heat budget.

Fig. 1 is a plot of Eq. (7) for various values of ϕ with $C_H/C_E = 1$. The figure shows that both humidity and ϕ play crucial roles in determining whether or not there is surface melting. Suppose, for example, that $\phi = 0.4$ in both polar regions and that the humidities have typical springtime values—80% in the Arctic and 60% in the Antarctic. Melting could then begin in the Arctic at an air temperature of -1.3°C, but the temperature would have to be 0°C before melting could begin in the Antarctic. Because the air is dryer in the Antarctic, the surface can tolerate higher air temperatures without melting: rapid sublimation supplements the minimal loss of energy due to the sensible heat flux.

Observations and our computations suggest, however, that it is unlikely the ϕ values in the Arctic and the Antarctic are the same. For a probable value of $\phi = 0.5$ in the Arctic and a relative humidity of 80%, melting could begin at an air temperature of -1.9°C. But with the probable Antarctic value of $\phi = 0.3$ and a relative humidity of 60%, melting would begin only when $T_a = 0.8$°C. Hence, the humidity difference between the Arctic and the Antarctic accounts for about 1.3°C of the 2.7°C difference between the air temperatures at the onset of melting; the likely difference in ϕ values is responsible for the additional 1.4°C temperature difference.

For melting to occur with these probable ϕ values, the surface-layer air temperature in the Antarctic must not only be substantially higher than in the Arctic, it must also be above 0°C. We believe this condition that T_a be above 0°C is sufficient to preclude surface melting in the Antarctic. With the sea-ice surface fixed at 0°C and because the ubiquitous Antarctic inversion assures a stable air column and so inhibits downward mixing of the warmer air aloft, the surface-layer air temperature should rarely be above 0°C. With the energy budget requirement that $T_a \geqslant 0.8$°C, melt features are, consequently, rare on Antarctic sea ice.

It may be easier to understand the physics of the ablation season with the aid of the Bowen ratio B—the ratio of sensible to latent heat fluxes. The dashed lines in Fig. 1 delimit different Bowen ratio regions. In region I, both F_H and F_E are negative, so $B = F_H/F_E$ is positive; in region II F_H is negative and F_E is positive, so B is negative; in region III both turbulent fluxes are positive, so again B is positive. Clearly, it would be very rare for springtime melting to start in the presence of a negative latent heat flux; only near the ice edge would the requisite warm, moisture-laden air be available. The general conditions for the onset of melting in both regions are a positive radiation balance, a positive flux of latent heat, and a negative to slightly positive sensible heat flux (cf. Langleben, 1966).

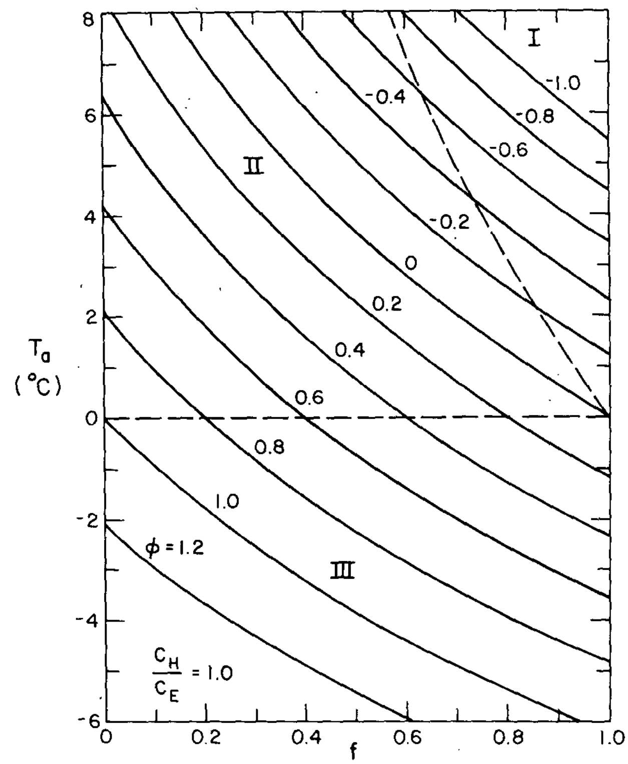

FIG. 1. The relationship between relative humidity f and air temperature T_a for various values of ϕ according to Eq. (7). $C_H/C_E = 1$. The dashed lines indicate the limits of three possible Bowen ratio regions. In Region I both F_H and F_E are downward, so $B > 0$; in Region II F_H is downward and F_E is upward, so $B < 0$; and in Region III both F_H and F_E are upward, so again $B > 0$.

Although in Fig. 1 we have used $C_H/C_E = 1$ for the surface energy budget computations, there are really no good measurements over sea ice to support this choice. The few simultaneous measurements of C_H and C_E over ice and snow are inconclusive. Hicks and Martin (1972) found $C_H/C_E \approx 2.5$ from measurements over snow on Lake Mendota, while Thorpe *et al.* (1973) obtained $C_H/C_E \sim 0.5$ during the AIDJEX Pilot Study on the Arctic Ocean. There is theoretical and experimental evidence that $C_H/C_E < 1$ over the ocean (Friehe and Schmitt, 1976; Francey and Garratt, 1978; Liu *et al.*, 1979; Andreas, 1980), and this inequality may be valid for other fairly homogeneous surfaces, like sea ice. In Figs. 2 and 3 we show Eq. (7) plotted for $C_H/C_E = 0.5$ and $C_H/C_E = 2.0$, respectively. Because the limits of the Bowen ratio regions shown in Fig. 1 do not depend on C_H/C_E, these limits also apply in Figs. 2 and 3.

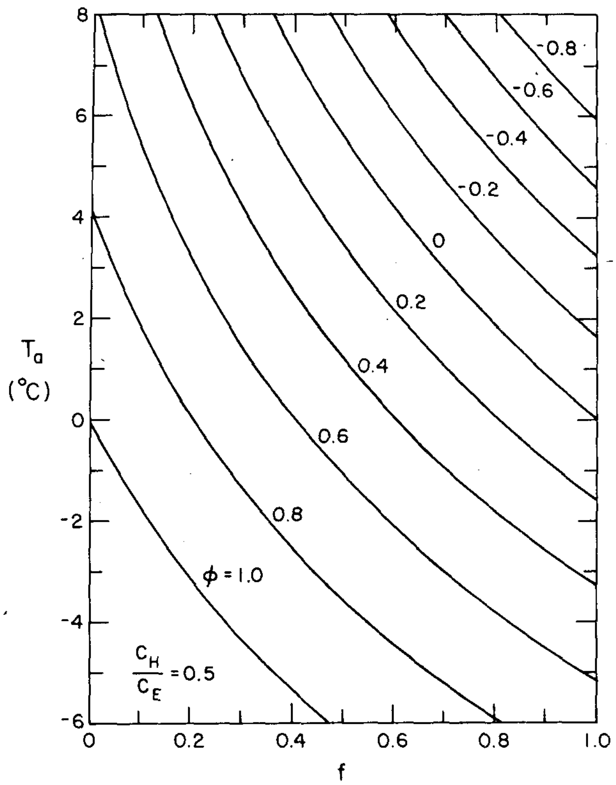

FIG. 2. As in Fig. 1 except $C_H/C_E = 0.5$.

On comparing the three figures we see that the ratio of bulk transfer coefficients may be as important as f and ϕ in setting the temperature for surface melting. If $C_H/C_E = 0.5$, and again $\phi = 0.5$ and $f = 0.8$, sea ice in the Arctic would start melting in an air temperature of $-2.8°C$; but in the Antarctic, with $\phi = 0.3$ and $f = 0.6$, the ice would not melt until the air temperature averaged 1.1°C. That is now a 3.9°C air temperature difference, and T_a is even farther above 0°C in the Antarctic. Conversely, if $C_H/C_E = 2.0$, Arctic sea ice would begin melting at $-1.2°C$, while Antarctic ice would start melting at an air temperature of only 0.4°C—a 1.6°C temperature difference. Thus, a small value of C_H/C_E augments differences between Arctic and Antarctic surface energy budgets, while a large C_H/C_E ratio moderates them.

4. Discussion

The relative humidities typical of the Arctic and the Antarctic must be responsible in large part for the difference in the sea-ice surfaces between the two regions during their respective ablation periods. The probable disparity in ϕ values—due mainly to wind speed differences—amplifies the effects of this humidity difference. Other meteorological parameters might also have non-negligible effects on the surface energy budgets through their influence on C_H and C_E. Neither theory nor the data base for polar regions is sufficient yet to isolate these lower-order effects, but perhaps we can, at least, focus attention on plausible relationships and needed measurements.

Brutsaert (1975) has developed a theory for the surface transfer of heat and moisture in a horizontally homogeneous flow. His basic equation for the transfer coefficients over a smooth surface is

$$C_S = C_D^{1/2}(13.6N^{2/3} + C_D^{-1/2} - 13.5)^{-1}; \quad (19)$$

over a rough surface it is

$$C_S = C_D^{1/2}(7.3\ \mathrm{Re}_*^{1/4}N^{1/2} + C_D^{-1/2} - 5)^{-1}. \quad (20)$$

Here C_S is the bulk transfer coefficient for the scalar, i.e., either C_H or C_E. C_D is the drag coefficient, N the Prandtl (for C_H) or Schmidt (for C_E) number, and $\mathrm{Re}_* = u_*z_0/\nu$ the roughness Reynolds number, where u_* is the friction velocity, z_0 is the roughness length, and ν is the kinematic viscosity of air. The surface is judged smooth when $\mathrm{Re}_* \leq 0.13$ and rough when $\mathrm{Re}_* > 2$.

Brutsaert's (1975) theory also predicts C_D; but since actual measurements of C_D over sea ice are available, let us use these in Eqs. (19) and (20).

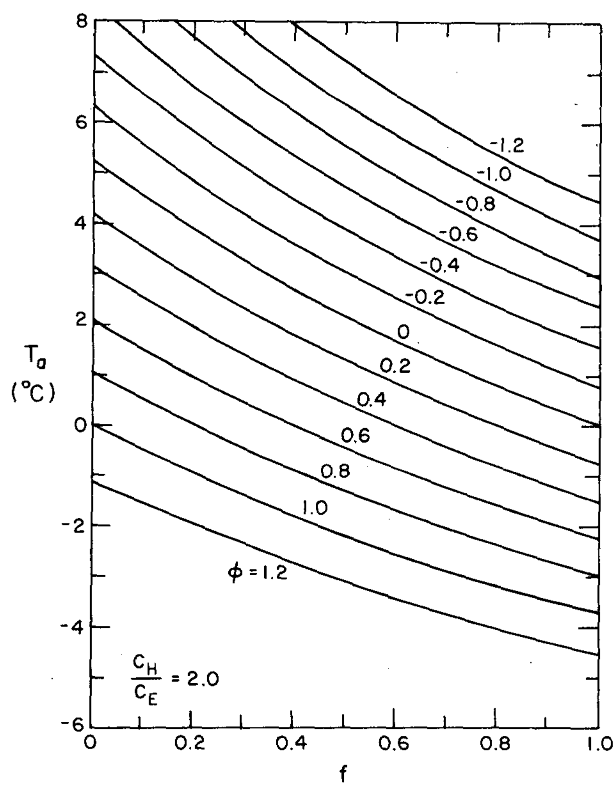

FIG. 3. As in Fig. 1 except $C_H/C_E = 2.0$.

Banke *et al.* (1980; see also Langleben, 1972; Banke and Smith, 1973; Banke *et al.*, 1976) reported that sea-ice surface roughness, as parameterized by the variance of measured surface elevation, was correlated with the drag coefficient. This recognition that the drag coefficient depends on the ice characteristics helps explain the wide range of drag coefficients measured over sea ice (Banke and Smith, 1971, 1973; Langleben, 1972; Thorpe *et al.*, 1973; Banke *et al.*, 1976, 1980; Leavitt *et al.*, 1977). Let us use C_D values from the lower and upper ends of the range of measured values to investigate how the bulk transfer coefficients computed with Brutsaert's (1975) model depend on C_D.

Table 2 lists the results of that computation for C_D values characteristic of smooth ($C_D = 1.2 \times 10^{-3}$) and rough ($C_D = 2.4 \times 10^{-3}$) sea ice and for wind speeds typical of spring in the Arctic (5 m s^{-1}) and in the Antarctic (10 m s^{-1}). The model predicts that C_H/C_E is $\sim$0.97 and that it depends only weakly on wind speed and drag coefficient. According to the model of Liu *et al.* (1979), for transfer over the ocean C_H/C_E is slightly smaller but again changes little with wind speed or drag coefficient. Evidently, the effects of wind speed and drag coefficient on the C_H/C_E ratio are not responsible for significant differences between the Arctic and Antarctic surface energy budgets. The actual C_H/C_E value may be different than Brutsaert's (1975) model predicts, but it is unlikely that C_H/C_E will be outside the interval [0.77, 1.00] (Friehe and Schmitt, 1976; Francey and Garratt, 1978; Andreas, 1980). Remember that a C_H/C_E value less than 1 fosters differences between Arctic and Antarctic ablation processes (Fig. 2).

Though variations in the wind speed and drag coefficient have negligible effects on the C_H/C_E ratio, they do lead to significant changes in the individual C_H and C_E values (Table 2). Since variations in the drag coefficient are tied to ice roughness, these scalar transfer coefficients may thus be different in the Arctic than in the Antarctic. From laser profile data Hibler *et al.* (1974; also Hibler, 1975) defined three sea-ice ridging provinces in the Arctic Ocean, with the Beaufort and Chukchi Seas making up the province of lightest ridging (of smoothest ice). Because Arctic sea ice, in general, is rougher than that found in the Beaufort and Chukchi Seas (W. D. Hibler III, pers. commun., 1981), measurements of the drag coefficient over sea ice, most of which have been made in the Beaufort and Chukchi Seas, are likely biased toward lower values. We consequently believe that a value of C_D at the upper limit of those reported is most representative of the entire Arctic Ocean; with $C_D = 2.4 \times 10^{-3}$ and a wind speed of 5 m s^{-1}, the value of C_E would be $\sim 1.6 \times 10^{-3}$.

TABLE 2. Predictions of the bulk transfer coefficients for heat and moisture using Brutsaert's (1975) model. The drag coefficients used are at the lower and upper ends of the range of measured values. A 5 m s^{-1} wind is typical of the Arctic; a 10 m s^{-1} wind, of the Antarctic.

	C_D			
	1.2×10^{-3}		2.4×10^{-3}	
U (m s^{-1})	5	10	5	10
Re_*	smooth	2.52	52.5	105
$10^3 C_H$	1.32	1.09	1.53	1.39
$10^3 C_E$	1.37	1.11	1.58	1.44
C_H/C_E	0.96	0.98	0.97	0.97

Similar laser sea-ice profile measurements are not yet available from the Antarctic; but since most Antarctic sea ice is not constrained by land masses, it seems likely to be smoother, in general, than Arctic ice. This intuitive evaluation is consistent with the locations of the Arctic ridging provinces delineated by Hibler *et al.* (1974)—the roughest ice being just north of the Canadian Archipelago, the smoothest being in the center of the Canadian Basin. A low value of C_D therefore seems appropriate for the Antarctic; with $C_D = 1.2 \times 10^{-3}$ and a wind speed of 10 m s^{-1}, the Antarctic value of C_E would be $\sim 1.1 \times 10^{-3}$. A difference in C_E values between the Arctic and Antarctic of 30–50% is thus not unreasonable.

This difference in C_E values would lessen differences between the Arctic and the Antarctic. The ratio

$$\phi_N/\phi_S = (Q_{nN}/Q_{nS})(C_{ES}/C_{EN})(U_S/U_N), \quad (21)$$

where subscript N (north) denotes the Arctic and S (south) the Antarctic, is the important parameter in evaluating how the ϕ values affect the air temperature difference between the two regions at the onset of melting. For example, with our first estimate, $\phi_N/\phi_S = 1$, relative humidity and the C_H/C_E ratio alone determined this air temperature difference. Our next estimate, $\phi_N/\phi_S \approx U_S/U_N$, was in the interval [1.6, 2.0] and so roughly doubled the temperature difference resulting from humidity and C_H/C_E effects alone. Finally, if $C_{ES}/C_{EN} \approx 0.7$ as we suggest above, $\phi_N/\phi_S \approx (C_{ES}/C_{EN})(U_S/U_N)$ is in the interval [1.1, 1.4]. The presumed difference in C_E values between the two regions would, therefore, moderate the effects due to the disparity in wind speed and humidity.

In summary, there seem to be plausible mechanisms to amplify the effect humidity differences have on Arctic and Antarctic ablation seasons; but mechanisms to attenuate potential differences also seem probable. Ultimately, better data are necessary to sort out which of these effects are determinant and which seem important mathematically but are inoperative practically. Measurements of wind speed, air and surface temperature, humidity, net radiation, surface roughness and the turbulent fluxes must be coincident with observations of surface conditions.

5. Conclusions

Melt ponds on the sea ice, which are characteristic of the Arctic ablation season, have rarely, if ever, been observed in the Antarctic. This observational result implies that the surface radiation budgets in the Arctic and the Antarctic cannot be parameterized by the same function of season and air and surface temperatures: albedos of the two regions will be different during the ablation season.

We have investigated this difference in Arctic and Antarctic ablation patterns by considering the energy budgets in the two regions just as melting begins. Melting will start in the Antarctic only when the surface-layer air temperature is significantly above 0°C, a requirement rarely met over Antarctic sea ice. In the Arctic, in contrast, melting can occur with the air temperature well below 0°C. The lower relative humidity in the Antarctic, which facilitates surface sublimation, is largely responsible for the differences in the energy budgets. Disparities in the effective radiation parameter ϕ, resulting primarily from its wind speed dependence, also contribute substantially to the regional differences. A value of C_H/C_E less than 1, a value with theoretical justification, would augment these humidity and ϕ effects. Wind speed and surface roughness differences, through their correlation with the bulk transfer coefficients, seem to moderate the differences. Until micrometeorological measurements are made over Antarctic sea ice at other than coastal sites, however, we can only speculate on the magnitude of these second-order effects.

Acknowledgments. We would like to thank William D. Hibler III and George D. Ashton for thoughtful reviews. Comments by J. W. Deardorff and the two *JAS* reviewers were also very helpful. Sandy Smith's typing was, as always, fast and accurate. This research was supported by the Department of the Army through Project 4A161102AT2403 and by NSF with contract DPP80-06922, Air-Sea Interaction and Sea-Ice Studies of the Joint Weddell Polynya Expedition.

REFERENCES

Ackley, S. F., 1979: Mass-balance aspects of Weddell Sea pack ice. *J. Glaciol.*, **24,** 391–405.

Andreas, E. L., 1980: Estimation of heat and mass fluxes over Arctic leads. *Mon. Wea. Rev.*, **108,** 2057–2063.

Arctowski, H., 1908: Les glaces: glace de mer et banquises. *Résultats du Voyage du S.Y. Belgica en 1897–1898–1899, Rapports Scientifiques*, Vol. 5, J. E. Buschmann, Antwerp, 3–55. [Trans., NTIS AD 881 363].

Banke, E. G., and S. D. Smith, 1971: Wind stress over ice and over water in the Beaufort Sea. *J. Geophys. Res.*, **76,** 7368–7374.

——, and ——, 1973: Wind stress on Arctic sea ice. *J. Geophys. Res.*, **78,** 7871–7883.

——, —— and R. J. Anderson, 1976: Recent measurements of wind stress on Arctic sea ice. *J. Fish. Res. Board Can.*, **33,** 2307–2317.

——, —— and ——, 1980: Drag coefficients at AIDJEX from sonic anemometer measurements. *Sea Ice Processes and Models*, R. S. Pritchard, Ed., University of Washington Press, 430–442.

Brower, W. A., Jr., H. W. Searby, J. L. Wise, H. F. Diaz and A. S. Prechtel, 1977: *Climate Atlas of the Outer Continental Shelf Waters and Coastal Regions of Alaska*: Vol. III, *Chukchi-Beaufort Sea.* Arctic Environmental Information and Data Center, Anchorage, 409 pp.

Brutsaert, W., 1975: A theory for local evaporation (or heat transfer) from rough and smooth surfaces at ground level. *Water Resour. Res.*, **11,** 543–550.

Francey, R. J., and J. R. Garratt, 1978: Eddy flux measurements over the ocean and related transfer coefficients. *Bound.-Layer Meteor.*, **14,** 153–166.

Friehe, C. A., and K. F. Schmitt, 1976: Parameterization of air-sea interface fluxes of sensible heat and moisture by bulk aerodynamic formulas. *J. Phys. Oceanogr.*, **6,** 801–809.

Hibler, W. D., III, 1975: Characterization of cold-regions terrain using airborne laser profilometry. *J. Glaciol.*, **15,** 329–347.

——, 1980: Modeling a variable thickness sea ice cover. *Mon. Wea. Rev.*, **108,** 1943–1973.

——, S. J. Mock and W. B. Tucker III, 1974: Classification and variation of sea ice ridging in the western Arctic Basin. *J. Geophys. Res.*, **79,** 2735–2743.

Hicks, B. B., and H. C. Martin, 1972: Atmospheric turbulent fluxes over snow. *Bound.-Layer Meteor.*, **2,** 496–502.

Idso, S. B., 1980: On the apparent incompatibility of different atmospheric thermal radiation data sets. *Quart. J. Roy. Meteor. Soc.*, **106,** 375–376.

——, 1981: A set of equations for full spectrum and 8–14 μm and 10.5–12.5 μm thermal radiation from cloudless skies. *Water Resour. Res.*, **17,** 295–304.

Johnson, A., Ed., 1976: First data report. *AIDJEX Bull.*, **32,** 1–71.

Kondratyev, K. Ya., 1969: *Radiation in the Atmosphere.* Academic Press, 912 pp.

Langleben, M. P., 1966: On the factors affecting the rate of ablation of sea ice. *Can. J. Earth Sci.*, **3,** 431–439.

——, 1969: Albedo and degree of puddling of a melting cover of sea ice. *J. Glaciol.*, **8,** 407–412.

——, 1971: Albedo of melting sea ice in the southern Beaufort Sea. *J. Glaciol.*, **10,** 101–104.

——, 1972: A study of the roughness parameters of sea ice from wind profiles. *J. Geophys. Res.*, **77,** 5935–5944.

Leavitt, E., D. Bell, M. Clarke, R. Anderson and C. Paulson, 1977: Computation of air stress and sensible heat fluxes from surface layer profile data, AIDJEX, 1975. *AIDJEX Bull.*, **36,** 157–174.

List, R. J., 1963: *Smithsonian Meteorological Tables*, 6th ed. Smithsonian Institution, 527 pp.

Liu, W. T., K. B. Katsaros and J. A. Businger, 1979: Bulk parameterization of air-sea exchanges of heat and water vapor including the molecular constraints at the interface. *J. Atmos. Sci.*, **36,** 1722–1735.

Munn, R. E., 1966: *Descriptive Micrometeorology.* Academic Press, 245 pp.

Murray, F. W., 1967: On the computation of saturation vapor pressure. *J. Appl. Meteor.*, **1,** 203–204.

Nansen, F., 1897: *Farthest North*, Vols. I and II. Harper Brothers, 1181 pp.
Parkinson, C. L., and W. M. Washington, 1979: A large-scale numerical model of sea ice. *J. Geophys. Res.*, **84**, 311–337.
Pease, C. H., 1975: A model for the seasonal ablation and accretion of Antarctic sea ice. *AIDJEX Bull.*, **29**, 151–172.
Reed, R. K., 1977: On estimating insolation over the ocean. *J. Phys. Oceanogr.*, **7**, 482–485.
Schwerdtfeger, W., 1970: The climate of the Antarctic. *World Survey of Climatology*, Vol. 14, *Climates of the Polar Regions*, S. Orvig, Ed., Elsevier, 253–355.
Spichkin, V. A., 1966: Role of evaporation in the surface ablation of sea ice. *Sovetskaia Antarkticheskaia Ekspeditsiia, 1955, Informatsionnyi Biulleten 55*, Trans. in *Inf. Bull.*, **6**, 1967, 16–17.
Thorpe, M. R., E. G. Banke and S. D. Smith, 1973: Eddy correlation measurements of evaporation and sensible heat flux over Arctic sea ice. *J. Geophys. Res.*, **78**, 3573–3584.
van Loon, H., 1972: Cloudiness and precipitation in the Southern Hemisphere. *Meteorology of the Southern Hemisphere, Meteor. Monogr.*, No. 35, C. W. Newton, Ed., Amer. Meteor. Soc., 101–111.
Vowinckel, E., and S. Orvig, 1970: The climate of the North Polar Basin. *World Survey of Climatology*, Vol. 14, *Climates of the Polar Regions*, S. Orvig, Ed., Elsevier, 129–252.
Weller, G. E., 1968a: The heat budget and heat transfer processes in Antarctic plateau ice and sea ice. ANARE Sci. Rep. 102, Australian National Antarctic Research Expeditions, Department of External Affairs, Melbourne, 155 pp.
——, 1968b: Heat-energy transfer through a four-layer system: air, snow, sea ice, sea water. *J. Geophys. Res.*, **73**, 1209–1220.
Wordie, J. M., 1921: Shackleton Antarctic Expedition, 1914–1917: The natural history of pack ice as observed in the Weddell Sea. *Trans. Roy. Soc. Edinburgh*, **52**, 795–829.
Zillman, J. W., 1972: A study of some aspects of the radiation and heat budgets of the Southern Hemisphere ocean. Meteor. Study No. 26, Bureau of Meteorology, Department of the Interior, Canberra, 562 pp.